High-Energy Oxygen Phonon Modes and Superconductivity in $Ba_{1-x}K_xBiO_3$: An Inelastic-Neutron-Scattering Experiment and Molecular-Dynamics Simulation

C.-K. Loong

Intense Pulsed Neutron Source, Argonne National Laboratory, Argonne, Illinois 60439

P. Vashishta, R. K. Kalia, M. H. Degani, D. L. Price, J. D. Jorgensen, D. G. Hinks, B. Dabrowski, A. W. Mitchell, D. R. Richards, and Y. Zheng

Materials Science Division, Argonne National Laboratory, Argonne, Illinois 60439

(Received 21 March 1989)

Phonon densities of states of insulating $BaBiO_3$ and superconducting $Ba_{0.6}K_{0.4}BiO_3$ are determined by neutron-scattering experiments. The main peaks in $BaBiO_3$ occur at 35, 43, 63, and 71 meV. In $Ba_{0.6}K_{0.4}BiO_3$, the phonon spectrum softens and is comprised of two bands around 30 and 60 meV. Molecular-dynamics results, which are in good agreement with the experiment, reveal that the observed phonon peaks are due to oxygen vibrations. The softening of oxygen phonon modes around 30 and 60 meV is due to electron-phonon coupling, indicating that $Ba_{0.6}K_{0.4}BiO_3$ is a normal BCS superconductor.

PACS numbers: 74.70.Ya, 25.40.Fq, 63.20.Kr, 74.20.−z

The discovery of superconductivity[1,2] in $Ba_{1-x}K_xBiO_3$ at 30 K is of great interest because of the difference in the properties between this and the other high-T_c materials. This material has no copper and displays none of the antiferromagnetism common to other high-T_c materials. $Ba_{1-x}K_xBiO_3$ is cubic in the superconducting phase,[3] whereas the other high-T_c materials have distinctly planar (Cu-O) structures. In contrast to $YBa_2Cu_3O_{7-\delta}$ which shows a negligible oxygen-isotope effect,[4] the measurements by Hinks *et al.*[5] indicate a substantial isotope effect, $T_c \sim M^{-\alpha}$ with $\alpha = 0.4$ for $Ba_{1-x}K_xBiO_3$. Batlogg *et al.*[6] find a smaller value of α (0.2). Infrared measurements[7] reveal a superconducting gap ($2\Delta = 70$ cm^{-1}) with $2\Delta/k_BT_c \approx 3.5$. Since there is no evidence for magnetic fluctuations and the transition temperature is not so high that one has to invoke an exotic mechanism, it is quite possible that phonon coupling between carriers is responsible for superconductivity in $Ba_{1-x}K_xBiO_3$.

In this Letter, we report the first inelastic-neutron-scattering measurement of the phonon density of states for $BaBiO_3$ and superconducting $Ba_{1-x}K_xBiO_3$. In the latter, the density of states consists of broad bands around 30 and 60 meV. A comparison with the density of states of insulating $BaBiO_3$ shows that phonon softening of ~ 5 meV occurs in the superconducting material. We also report the results of the first molecular-dynamics (MD) simulation for the phonon densities of states of these two materials. The MD results are in good agreement with all the peaks observed in $BaBiO_3$. In $Ba_{1-x}K_xBiO_3$, the simulation shows a shift of the spectrum toward lower energies and a broadening due to K disorder, which is in agreement with the neutron experiment. From the MD calculations it is also clear that the peaks between 20 and 80 meV in both materials are due to vibrations of oxygen atoms. The observed softening of oxygen phonons in superconducting $Ba_{1-x}K_xBiO_3$ is due to electron-phonon coupling.

$BaBiO_3$ and $Ba_{0.6}K_{0.4}BiO_3$ samples were prepared by a melt-processing technique.[8] The starting material was $BaBiO_3$ (synthesized from $BaCO_3$ and Bi_2O_3) and the required amounts of KO_2 and Bi_2O_3 were added for $x = 0.4$ composition. The oxide mixtures were melted in a Pt crucible in air and quenched into room-temperature molds. The $x = 0$ cast material was subsequently O_2 annealed for 24 h at 900 °C and slowly (48 h) cooled to room temperature. The $x = 0.4$ case material, without being exposed to air, was N_2 fired for 1 h at 725 °C and quenched to room temperature. It was subsequently O_2 annealed for 1 h at 450 °C and slowly (at 2 °C/min) cooled to room temperature. The $x = 0.4$ sample is superconducting with the resistive superconducting transition temperature $T_c(50\%) = 26.4$ K and the transition width $\Delta T_c(10\%\text{–}90\%) = 1.5$ K.

Inelastic-neutron-scattering experiments were performed on the LRMECS chopper spectrometer at the Argonne Intense Pulsed Neutron Source. The pulsed-source neutron-chopper spectrometer[9] enables measurement of inelastic scattering using time-of-flight techniques over a wide range of momentum and energy transfer ($\hbar Q, E$). The energy resolution (FWHM) varies from 8% of the incident energy in the elastic region to about 5% near the end of the neutron energy-loss spectrum.

Polycrystalline samples of $Ba_{0.6}K_{0.4}BiO_3$ (86 g) and $BaBiO_3$ (100 g), contained in aluminum planar cells, were mounted at a 45° angle to the incident neutron beam so as to minimize multiple scattering. To reduce multiphonon scattering, the samples were cooled and controlled at 15 K. Background scattering was subtracted from the data by using empty-container runs. Measurements of elastic incoherent scattering from a vanadi-

um standard provided detector calibration and intensity normalization.

The generalized energy distribution function, $G(Q,E)$, in the neutron energy-loss spectrum, is defined by

$$G(Q,E)=\frac{2m}{\hbar^2}\frac{n(E)+1}{Q^2}Ee^{2W(Q)}S(Q,E), \quad (1)$$

where M is a mean sample mass, $W(Q)$ is the Debye-Waller factor, $n(E)$ is the Bose-Einstein distribution function, and $S(Q,E)$ is the dynamic structure factor. It has been shown[10] that in inelastic neutron coherent scattering from nonmagnetic polycrystalline materials, $G(Q,E)$ provides a measure of the phonon density of states (DOS) if Q is considerably larger than the dimension of the Brillouin zone.

With an incident neutron energy of 120 meV, $S(Q,E)$ spans Q between 1 and 12 Å^{-1}. For $BaBiO_3$ and $Ba_{0.6}K_{0.4}BiO_3$, $S(Q,E)$ are shown in Fig. 1. We obtain a generalized phonon DOS, $G(E)$, from $G(Q,E)$ by averaging the data over Q between 5 and 9 Å^{-1}. Data below 10 meV cannot be determined accurately because of elastic scattering in this region.

Molecular-dynamics calculations were performed with effective interparticle interactions which include steric repulsions between atoms, Coulomb interactions due to charge transfer, and charge-dipole interactions to describe the polarization effects. The calculations were done for orthorhombic $BaBiO_3$ and cubic $Ba_{0.6}K_{0.4}BiO_3$ at the experimental number density. The $Ba_{0.6}K_{0.4}BiO_3$ system was obtained from $BaBiO_3$ by randomly replacing 40% of the Ba atoms with K atoms. The phonon DOS was calculated by (1) diagonalization of the dynamical matrix, (2) the equation-of-motion approach,[11] and (3) Fourier transformation of the velocity autocorrelation functions. The results of these three calculations are in satisfactory agreement with one another. The partial DOS are weighted suitably by neutron-scattering cross sections of the elements to obtain appropriate total DOS for comparison with neutron measurements.

For $BaBiO_3$, Figs. 2(a) and 2(b) display the phonon DOS from neutron scattering and MD simulation, respectively. The experiment shows prominent peaks at 35, 43, 63, and 71 meV. In addition, there is an indication of a shoulder at 24 meV and weak features in the region of 50–58 meV. In the MD results, we find peaks at 25, 32, 37, 45, 51, 60, 66, and 74 meV. Because of limited resolution of the neutron measurements, the MD peaks at 32 and 37 meV are observed experimentally as a single peak at 35 meV. Similarly, the MD peaks at 60 and 66 meV appear as a single peak at 63 meV in the neutron experiment. Note that there are two additional peaks at 11 and 16 meV in the MD results. These peaks are not observed in the neutron measurements because of low-energy cutoffs.

To understand the origin of the peaks in the DOS, we

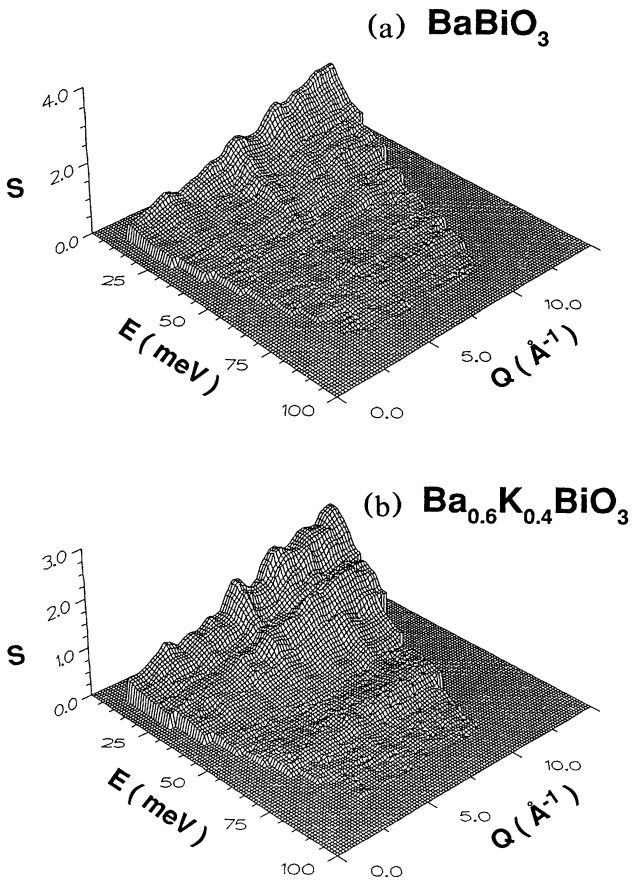

FIG. 1. Experimental dynamic structure factor, $S(Q,E)$, in (a) $BaBiO_3$ and (b) $Ba_{0.6}K_{0.4}BiO_3$.

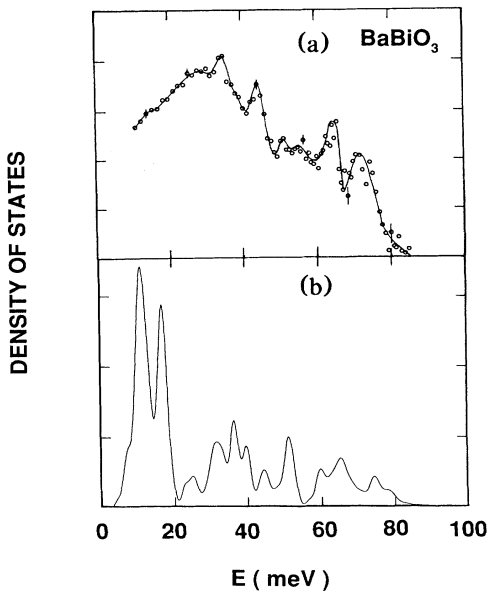

FIG. 2. Phonon DOS for $BaBiO_3$: (a) experiment (open circles; the line is a guide to the eye) and (b) MD simulation.

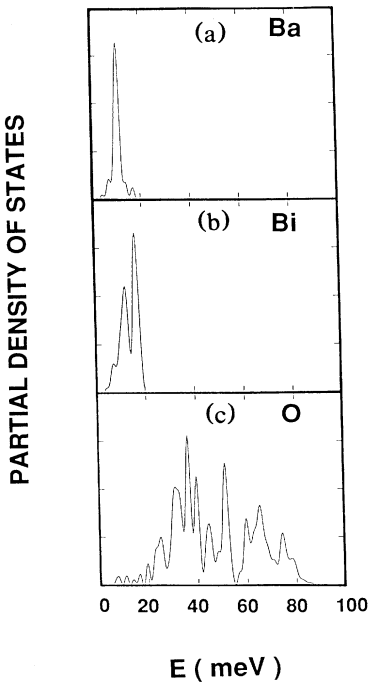

FIG. 3. MD partial DOS for (a) Ba, (b) Bi, and (c) O in $BaBiO_3$.

examine the MD results for partial phonon DOS in Fig. 3. There is a clear dilineation in the peaks associated with Ba and Bi on one hand and O on the other. For Ba there is only one main peak at 11 meV, whereas for Bi there are two peaks at 12 and 17 meV. Clearly, in the total DOS [Fig. 2(b)] the peak at 11 meV is due to both Ba and Bi and the peak at 16 meV is due to Bi alone. Above 20 meV the entire spectrum arises from oxygen vibrations.

For $Ba_{0.6}K_{0.4}BiO_3$ the phonon DOS are shown in Fig. 4(a) (neutron) and 4(b) (simulation). Neutron measurements reveal that K doping broadens the peaks due to disorder caused by random substitution of K on Ba sites and also shifts the DOS toward lower energies. Because of broadening, only two bands at 30 and 60 meV remain in $Ba_{0.6}K_{0.4}BiO_3$. An overall broadening of the peaks and a shift toward lower energies are also evident from the MD results shown in Figs. 2(b) and 4(b). There are four significant features in Fig. 4(b): (1) a band extending from 25 to 37 meV, (2) a peak around 51 meV, (3) a band between 54 and 65 meV, and (4) small peaks at 67 and 73 meV. In addition, there are small features at 25 and 46 meV. The simulation also shows peaks at 11 and 15 meV, whereas only a shoulder at 16 meV is visible experimentally. Higher-resolution neutron measurements may reveal the additional features observed in the simulation.

For $Ba_{0.6}K_{0.4}BiO_3$, the partial DOS from simulation are shown in Fig. 5. As in the case of $BaBiO_3$, the peaks above 20 meV are due to oxygen vibrations. It is clear

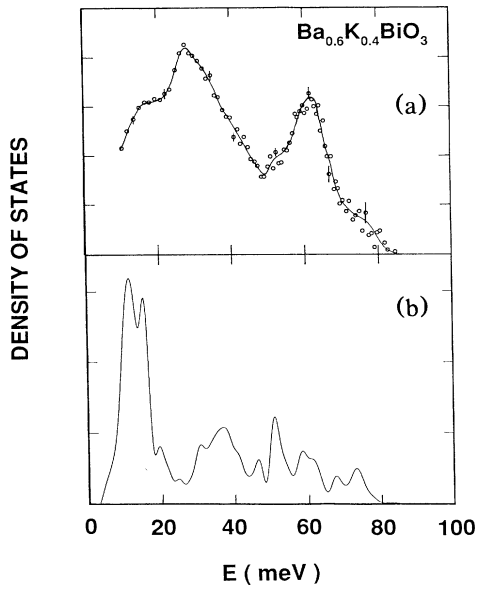

FIG. 4. Phonon DOS for $Ba_{0.6}K_{0.4}BiO_3$: (a) experiment (the line is a guide to the eye) and (b) MD simulation.

from the partial DOS for oxygen in $BaBiO_3$ [Fig. 3(c)] and $Ba_{0.6}K_{0.4}BiO_3$ [Fig. 5(d)] that there is an overall broadening and softening of the peaks in $Ba_{0.6}K_{0.4}BiO_3$. The main peak in the K partial DOS is at 20 meV and it strongly overlaps with the second peak at 16 meV in the Bi partial DOS. In the total DOS, the contributions from Ba, K, and Bi give rise to peaks around 11 and 15 meV.

It is clear from neutron measurements and MD simulation that the oxygen-phonon modes soften by roughly 5 MeV with 40% K doping of $BaBiO_3$. The softening

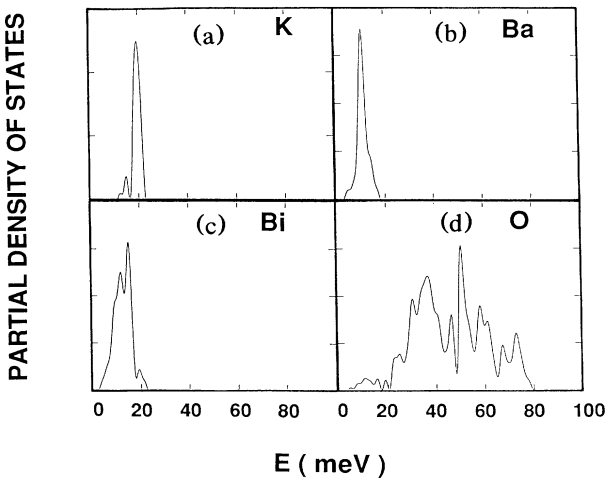

FIG. 5. MD partial DOS for (a) K, (b) Ba, (c) Bi, and (d) O in $Ba_{0.6}K_{0.4}BiO_3$.

occurs for the following reason: With the substitution of Ba by K, it has been found experimentally[12] that there are holes on the oxygen $2p$ orbitals which screen the charge on oxygen anions. Since the scale of energy is determined by the charge on oxygen, a reduction due to screening lowers the energy of these modes. Neutron measurements and the MD simulation also suggest that the strongest phonon features in superconducting $Ba_{0.6}K_{0.4}BiO_3$ occur around 30 and 60 meV. In recent tunneling measurements,[13] the strongest features are also observed near 30 and 60 meV. Thus, the cumulative evidence from MD simulation and neutron and tunneling measurements suggests that the coupling of electrons to 30- and 60-meV oxygen phonons is responsible for superconductivity in $Ba_{0.6}K_{0.4}BiO_3$. The coupling to these phonon modes can also explain the observed oxygen-isotope effect.[5]

We thank Dr. J. Zasadzinski for informing us about his tunneling results. This work was supported by the U.S. DOE, Basic Energy Sciences–Materials Sciences, under Contract No. W-31-109-ENG-38. The simulations were done on the Energy Research Cray Supercomputer at the National Magnetic Fusion Energy Computing Center (Livermore). D.R.R. and M.H.D. would like to thank American Air Liquide, Inc., and Fundacão de Amparoe Pesquisa do Estado de São Paulo (FAPESP), Brazil, respectively, for their support.

[1]L. R. Mattheiss, E. M. Gyorgy, and D. W. Johnson, Jr., Phys. Rev. B **37**, 3745 (1988).

[2]R. J. Cava, B. Batlogg, J. J. Krajewski, R. Farrow, L. W. Rupp, Jr., A. E. White, K. Short, W. F. Peck, and T. Kometani, Nature **332**, 814 (1988).

[3]D. G. Hinks, B. Dabrowski, J. D. Jorgensen, A. W. Mitchell, D. R. Richards, Shiyou Pei, and Donglu Shi, Nature **333**, 836 (1988).

[4]D. E. Morris, R. M. Kuroda, A. G. Markelz, J. H. Nickel, and J. Y. T. Wei, Phys. Rev. B **37**, 5936 (1988), and references therein.

[5]D. G. Hinks, D. R. Richards, B. Dabrowski, D. T. Marx, and A. W. Mitchell, Nature **335**, 419 (1988).

[6]B. Batlogg, R. J. Cava, L. W. Rupp, Jr., A. M. Mujsce, J. P. Remeika, W. F. Peck, Jr., A. S. Cooper, and G. P. Espinosa, Phys. Rev. Lett. **61**, 1670 (1988).

[7]Z. Schlesinger, R. T. Collins, J. A. Calise, D. G. Hinks, A. W. Mitchell, Y. Zheng, and B. Dabrowski (to be published).

[8]D. G. Hinks, A. W. Mitchell, Y. Zheng, D. R. Richards, and B. Dabrowski, Appl. Phys. Lett. (to be published).

[9]C.-K. Loong, S. Ikeda, and J. M. Carpenter, Nucl. Instrum. Methods Phys. Res., Sect. A **260**, 381 (1987).

[10]M. M. Bredov, B. A. Kotov, N. M. Okuneva, V. S. Oskotskii, and A. L. Shakh-Budagov, Fiz. Tverd. Tela (Leningrad) **9**, 267 (1967) [Sov. Phys. Solid State **9**, 214 (1967)]; V. S. Oskotskii, Fiz. Tverd. Tela (Leningrad) **9**, 550 (1967) [Sov. Phys. Solid State **9**, 420 (1967)].

[11]D. Beeman and R. Alben, Adv. Phys. **26**, 339 (1977).

[12]E. Alp (private communication).

[13]J. Zasadzinski (private communication).